Iranian Journal of Physics Research, Vol. 23, No. 3, 2023
DOI: 10.47176/ijpr.22.3.21798

Integrated plasma control system for IR-T1 tokamak with disruption mitigation

A Naghidokht[1*], M Janfaza [1], and M Ghoranneviss [2]
1. School of Physics, Damghan University, Damghan, Iran
2. Plasma Physics Research Center, Islamic Azad University, Science and Research Branch, Tehran, Iran

E-mail: a.naghidokht@du.ac.ir

(Received 7 December 2023 ; in final form 19 February 2024)

Abstract
Controlling tokamak plasmas is a complex process that is affected by structured uncertainties and unmodeled dynamics. To overcome these challenges and achieve a well-defined robust behavioral outcome, it is crucial to develop standard controllers. The decoupling control theory for Multiple-Input Multiple-Output (MIMO) processes is a powerful technique that allows the mitigation or elimination of undesirable cross-coupling terms in tokamaks, making it superior to the Single-Input Single-Output (SISO) control scheme. Our study proposes two types of controllers, PID-tuned and cascaded-robust controllers, that exploit decoupling and robustness for horizontal position and current control of plasma in IR-T1 tokamak. We compare the controllers through simulations and study the impact of changing the vertical field coil voltage on the cross-coupling of these two plasma parameters. The results demonstrate that the PID-tuned controller outperforms the robust controller in terms of meeting control requirements, disturbance rejection, reference value tracking, and disruption mitigation, especially in cross-coupling controls. Of course, the definitive confirmation requires experimental studies with more diverse conditions and, finally construction and operation of these controllers in tokamaks.

Keywords: IR-T1 tokamak, PID-tuned controller, cascaded-robust controller, cross-coupling, disruption mitigation

1. Introduction

The accurate control of plasma current and position during various discharging stages in tokamaks is crucial for stable and efficient operation while avoiding first-wall interactions. The design of the ITER poloidal field control system highlights the significance of equilibrium response modeling for controller design, which is based on a sufficiently accurate linear model of the available system [1-3]. For this purpose, Single-Input Single-Output (SISO) systems have been used to independently control each of these quantities in different tokamaks [4-7]. Due to engineering necessity, such as the need to minimize the number of costly, superconducting coils, restrictions on where coils can be located on the device, and practical power supply limitations, today's tokamaks will have functionally coupled sets of coils that contribute to both the Ohmic-heating (OH) flux for control of the plasma current, the vertical field (VF) for control of the plasma horizontal position, some other coils for plasma shape controls, etc. in contrast to the traditional way of grouping coils into 'decoupled' windings. As a result, plasma parameters such as current and horizontal position are strongly coupled; i.e. adjusting controller parameters of one control loop affects the performance of the others, which may even lead to system destabilization. These undesirable cross-coupling of the plasma parameters recommend the study of Multiple-Input Multiple-Output (MIMO) system for these parameters. Compared to the SISO counterpart, there is an interrelationship between input and output variables in MIMO systems. For those processes with tight coupling and stringent control requirements, decoupling control schemes are usually employed in MIMO processes [8,9]. The control design of MIMO control systems has been largely developed for linear systems. The usual framework in industrial control consists of using independent Proportional Integral Derivative (PID) loops with tuning technologies for SISO and MIMO processes [10-12]. PID controllers are a widely adopted feedback control system in various industrial settings that are designed to address minor deviations and promptly correct transient changes gradually. Despite the availability of newer control methods, these controllers, with the introduction of microprocessors and features such as automatic tuning and continuous adaptation , remain the most commonly employed feedback control method in industrial systems. Besides, the integration of PID control with other function blocks has resulted in the creation of more complex automation systems. Due to the nonlinear features with uncertain plasma parameters, robust MIMO controllers

are also suggested and developed to control different plasma parameters in ITER [13-15] and many other tokamaks such as TCV [16], D-III-D [17,18], EAST [19], and NSTX [20]. Hybrid controllers have also been proposed to improve performance and system robustness in tokamaks [21,22].

This study focuses on the design of an integrated control system for plasma current and horizontal position control in the IR-T1 tokamak. The paper is structured as follows: Section 2 presents the design of the Two-Input, Two-Output (TITO) control system utilized to control plasma horizontal position and plasma current. The decoupling and robustness of the control system are also discussed. Section 3 provides the corresponding simulations, including step response for the two controllers, and the design requirements for the robust controller. A particular case is also presented in this section to investigate the performance of the designed control systems. Section 4 is devoted to the results and discussion, and in section 5, the conclusion is provided.

2. Methods

This section describes the baselines of the work as follows. The model related to the Two-Input-Two-Output (TITO) system, which includes changes in horizontal position and plasma current, along with a transfer function is introduced. Additionally, transfer functions for the power supply of the vertical field and the central transformer (Ohmic) coils, as well as the appropriate PID controllers, have been presented. The implementation of PID controllers has been successfully used in various tokamaks, significantly enhancing stability and performance. Our previous work on the application of this type of controller for plasma horizontal position control in IR-T1 tokamak, Ref. [23], has given significant results, so as the first potential candidate for controlling the Two-Input-Two-Output (TITO) plasma parameters in this tokamak, the use of PID-tuned controllers will be considered.

Decoupling methods have been introduced for cross-coupling elimination, among which the inverted decoupling method is widely used, and we chose this method. So, in this study, the performance of the control system using a TITO PID-tuned controller and a newly introduced TITO cascaded robust controller against cross-coupling is investigated. The specific control requirements of the intended plasma are presented to tune the overall response of the system through PID controller coefficients,. Furthermore, the study compares the performance of the control system with the behavior of the introduced cascaded robust controller. Finally, the study delves into the mitigation or elimination of disruptions. The performance of the control system at the time of the occurrence of these disruptions is investigated based on the characteristic features of the plasma. The goal is to describe the design procedures, control requirements, and relevant data to enable readers to design a suitable controller for their specific application.

2.1. IR-T1 tokamak

IR-T1 is a small, Ohmically heated air-core tokamak without a copper shell and circular cross-section plasma. It has a major radius $R = 0.45$ m and a minor radius $a = 0.125$ m, the plasma current $I_p < 40$ kA, a toroidal magnetic field $B_t = 0.7 - 0.8$ T, average electron density $n = (0.30 - 1.50) \times 10^{19}\,\mathrm{m}^{-3}$, plasma discharge duration $\tau_d = 30 - 35$ ms and the electron temperature $T_e = 200$ eV. Further characteristics of IR-T1 are presented in table 1.

The exploration of Magneto-Hydro-Dynamic (MHD) behavior and structure is of utmost importance in tokamaks, providing us with information such as MHD activity, mode numbers, magnetic islands, and plasma instability. Different diagnostics are used for plasma edge studies. Among them, Mirnov coils are commonly used for recording magnetic fluctuations. These coils have simple designs and are easily accessible to researchers. In IR-T1 tokamak, there is a poloidal array of 12 external Mirnov coils located at a poloidal angle of 30 degrees to determine plasma mode numbers and also to extrac the power spectrum density. In fig. 1, we presented a view of the diagnostics (including Mirnov coils) and capacitors of this tokamak [23]. Fast Fourier Transform (FFT) analysis of Mirnov coil fluctuations is one of the effective methods to investigate the mode of tokamak plasma [24].

2.2. TITO control system of plasma current and plasma horizontal position in IR-T1 tokamak

First, we introduce the (linear) plasma response transfer function concerning changes in currents within the passive structures of the vessel and the active poloidal field coils. The plasma response transfer function for plasma current and horizontal position is obtained by using a linearized plasma-circuits model [25]:

$$\mathbf{L}^{*}\frac{d\mathbf{x}}{dt} + \mathbf{R}\mathbf{x} = \mathbf{u}, \tag{1}$$

with the $\vec{x} = \left[\delta\vec{I}, \delta\vec{I}_p\right]^T$, the input vector $\vec{u} = \left[\delta\vec{V}, 0\right]^T$, $\vec{I}$ the set of currents flowing in the external (active and passive) conductors, $\vec{R}$ the resistance matrix of the circuits, $\vec{V}$ the complete set of applied voltages, and the entries of $\vec{V}$ for the passive circuits are zero. Furthermore, the quantities $\delta\vec{I}$, $\delta\vec{I}_p$, and $\delta\vec{V}$ represent deviations from nominal (equilibria) values. The matrix $\mathbf{L}^{*} = \frac{\partial[\boldsymbol{\Psi}, \boldsymbol{\Psi}_p]^T}{\partial[\mathbf{I}, \mathbf{I}_p]^T}$ is the modified inductance matrix. eq. (1) can be converted into the classical state-space representation:

$$\frac{d\mathbf{x}}{dt} = \mathbf{A}\mathbf{x} + \mathbf{B}\mathbf{u}, \tag{2}$$

with $\mathbf{A} = -\mathbf{L}^{*-1}\mathbf{R}$ and $\mathbf{B} = \mathbf{L}^{*-1}$. A linearized model can also predict linearized output parameter changes $\mathbf{y}$, using the standard output equation:

$$\mathbf{y} = \mathbf{C}\mathbf{x} + \mathbf{D}\mathbf{u}, \tag{3}$$

Table 1. Characteristic parameters and corresponding values of IR-T1 tokamak.

Parameters	Value	Parameters	Value
β_p, Poloidal beta	1	Vertical field coil current (kA)	5
κ, Elongation	1	Plasma resistance ($m\Omega$)	1
δ, Triangularity	0	Vertical field coil-related resistance (Ω)	5
l_i, Internal inductance	1	Vacuum vessel resistance ($m\Omega$)	0.40
Major radius of vacuum vessel (m)	0.45	Number of vertical field coil turns	2
Minor radius of vacuum vessel (m)	0.16		

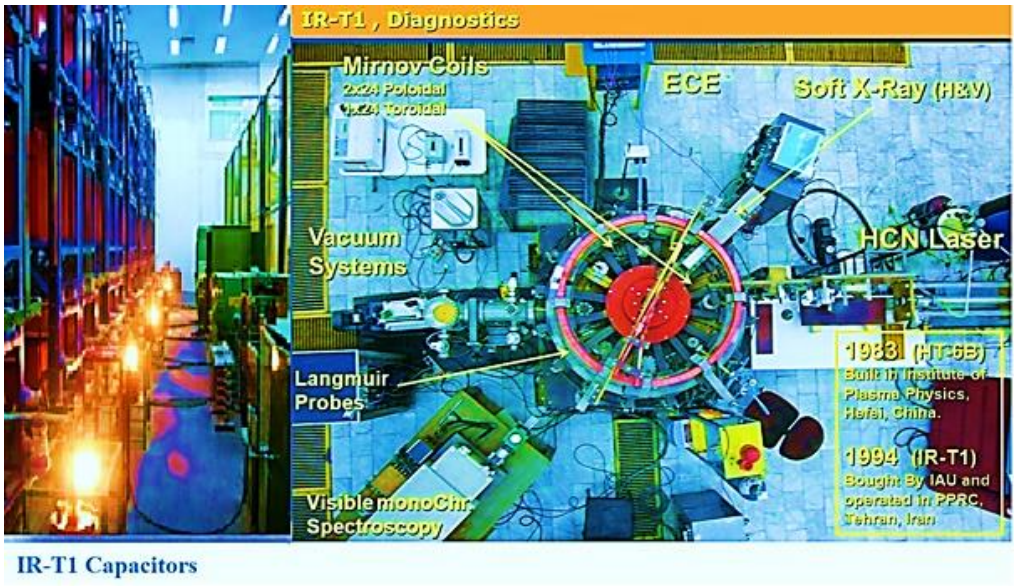

Figure. 1. Top view of IR-T1 tokamak diagnostics, right including: Mirnov coils, soft X-Ray detector, HCN laser, Langmuir probes, vacuum systems, visible monochromatic spectroscopy and Electron Cyclotron Emission (ECE) diagnostic; and left: array of capacitors as power supplies.

where **C** and **D** are the state-to-output and input-to-output matrices, respectively. We now extract from the above equations, the voltage-driven model coil current changes δx_a as follows:

$$\delta \dot{x}_a = -(R_a + \frac{R_p L_{pa}^*}{L_p^{*2}})(L_a^* - \frac{L_{pa}^* L_{ap}^*}{L_p^*})^{-1}\delta x_a + (L_a^* - \frac{L_{pa}^* L_{ap}^*}{L_p^*})^{-1}\delta u$$

$$\begin{pmatrix} \delta h \\ \delta I_p \end{pmatrix} = \begin{pmatrix} C \\ -\frac{L_{pa}^*}{L_p^*} \end{pmatrix} \delta x_a \quad , \tag{4}$$

that h is the horizontal displacement of the plasma centroid from the equilibrium. The subscripts a and p indicate active and plasma components, respectively. In the Laplace domain, the plasma response transfer function, $G_p(s) = C(sI - A)^{-1}B$ is calculated by considering the characteristic parameters for IR-T1 tokamak (table 1 in section 2.1) [23] and the tokamak circuit method presented by Ref. [26].

With the baselines provided, a PID-based feedback controller is designed for the vertical (central transformer) field coil. The performance request for the horizontal position control consists of a settling time smaller than 2 milliseconds with a tracking error of constant reference of 0.10 %, ensuring as well a disturbance rejection within 0.10 milliseconds (the cross-coupling within 5 milliseconds) whereas, for the current control loop, the requested settling time is 5 milliseconds including cross-coupling effects rejection. These control requirements have been met by tuning the proposed controllers using MATLAB simulations. Therefore, plasma current and horizontal position controls are conceivable in tokamak IR-T1, using a feedback closed-loop that includes the vertical coil power supply (for plasma horizontal position control) and central transformer coil power supply (for plasma current control). The transfer function for the power supply of the vertical coil and central transformer coil systems of IR-T1 tokamak, are approximated by first-order linear dynamical filters with given time delay and bandwidth, such as:

$$G_v(s) \cong K_v \frac{e^{-T_v s}}{s + a_v} \quad , \quad K_v \simeq 1 \quad , \quad T_v = 10\ \mu s \, ,$$

$$G_o(s) \cong K_o \frac{e^{-T_o s}}{s + a_o} \, , \quad K_o \simeq 1 \, , \quad T_o = 100\ \mu s \, , \tag{5}$$

where $(K_o)\ K_v$, $(T_o)\ T_v$ and $(a_o)\ a_v$ are respectively the gain, time delay and bandwidth related quantity for the central transformer coil (vertical coil) power supply whose values are determined by the system requirements [27].

Therefore, the final plasma response transfer function, $G_p(s)$, is obtained as:

$$G_p(s) = \begin{pmatrix} \frac{1.001s + 6.203\times10^{11}}{s^2 + (1.239\times10^{12})s + 3.84\times10^{23}} & \frac{-0.000511s - 3.167\times10^{8}}{s^2 + (1.239\times10^{12})s + 3.84\times10^{23}} \\ \frac{(9.15\times10^{-8})s + 5.67\times10^{4}}{s^2 + (1.239\times10^{12})s + 3.84\times10^{23}} & \frac{0.9992s + 6.192\times10^{11}}{s^2 + (1.239\times10^{12})s + 3.84\times10^{23}} \end{pmatrix}$$

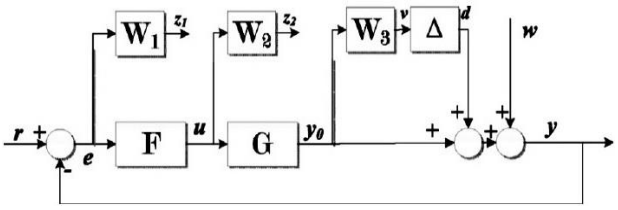

Figure. 2. Robustness analysis of augmented plant with un-modeled dynamics Delta. The W's are weight functions. Also, G is the linear model of the plant, *w* the output disturbances, u the control inputs, *y* plant outputs and controller inputs, z_i the performance output, and F is the controller.

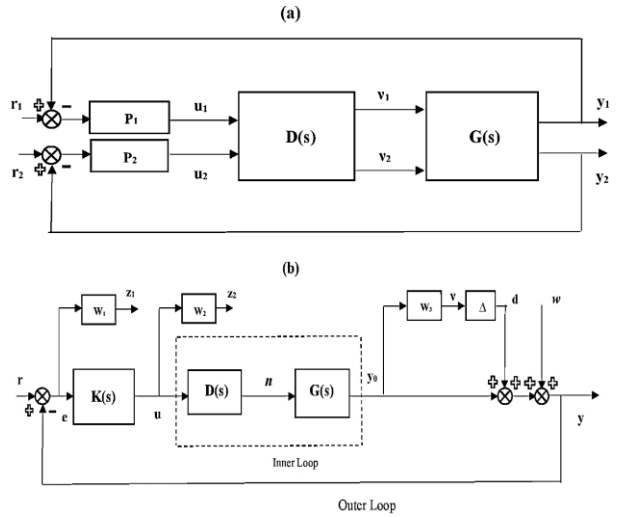

Figure. 3. Block diagram for controlling the structure of TITO processes with the decoupling matrix $D(s)$ by the designed (a) PID controller including P_1 and P_2 and (b) robust controller $K(s)$.

With the corresponding matrices:

$$A=\begin{pmatrix} -6.197\times10^{11} & 0 \\ 0 & -6.197\times10^{11} \end{pmatrix},$$

$$B=\begin{pmatrix} -1.584 & -6.08\times10^{-5} \\ -0.4981 & 0.6685 \end{pmatrix},$$

$$C=\begin{pmatrix} -0.6319 & -5.733\times10^{-5} \\ -0.4697 & 1.495 \end{pmatrix},\quad D=\begin{pmatrix} 0 & 0 \\ 0 & 0 \end{pmatrix},$$

With creating the related matrices for PID controllers and power supplies transfer functions, the overall TITO system transfer function is obtained as $G=G_p(s)G_{ps}(s)G_{PID}(s)$, (where $G_{ps}(s)$ refers to the specific power supplies transfer function) and then we can design a TITO PID-tuned controller to control plasma current and plasma horizontal position in this tokamak.

We can also design a robust controller to track reference values. The block diagram of the augmented plant for the design of the H_∞ robust controller is shown in fig. 2.

Here, G is the linear model of the plant under control (actuator, plasma in tokamak, and sensor). W_1, W_2 , and W_3 are weight functions used to model the error signal, the control signal, and the output signal, respectively. They need to be adjusted based on the system frequency characteristics. The design is performed ensuring closed-loop asymptotic stability. In this design, w is the output disturbances, u the control inputs, y plant outputs, and controller inputs. The performance outputs z_i are introduced for analyzing the closed-loop robustness of the plant to un-modelled (stable) dynamics $\Delta(s)$. Analysis of the H_∞ robust controller, $K(s)$, will be performed through the mixed sensitivity approach, by the norm optimization of H_∞ of the complete transfer function from disturbance w to output $[z^T \text{ and } v]^T$ [28]:

$$\min_{K(s)\text{ stabilizing}}\left\|\begin{pmatrix} W_1(s)S(s) \\ W_2(s)K(s)S(s) \\ W_3(s)N(s) \end{pmatrix}\right\| = \min_{K(s)\text{ stabilizing}}\|\Phi(s)\|_\infty \quad (6)$$

By definition, $S(s)$ as a sensitivity function (output), is related to anti-interference and system tracking capabilities. Also, $N(s)$, as a complementary sensitivity function (output), is involved with system robust stability:

$$S(s)=(I+GK)^{-1},\ R(s)=K(I+GK)^{-1},$$
$$N(s)=GK(I+GK)^{-1}. \quad (7)$$

Since $S(s)+N(s)=I$ (I is the unit matrix), we must therefore, choose a suitable design to achieve a good trade-off between these two functions. Here, the most specific first-order weighting functions have been considered. The selection of the weighted functions and their parameters in the augmented plant is performed by a trial-and-error methodology [29]. This repetition stops when the performance is acceptable. Since the norm H_∞ of function $\Phi(s)$ must be smaller than one, the following requirements must be met in the design of a robust controller (GAM is the smallest H_∞ norm):

$$\|S(s)\|_\infty < \frac{1}{\|W_1(s)\|_\infty},\ \|R(s)\|_\infty < \frac{1}{\|W_2(s)\|_\infty},$$
$$\|N(s)\|_\infty < \frac{1}{\|W_3(s)\|_\infty}, \quad (8)$$

The acceptable weight functions are obtained as:

$$W_1=\frac{0.015\,s+0.75}{5\,s+10},\ W_2=1.0\times10^{-6},\ W_3=\frac{0.6\,s+0.2}{0.025\,s+1},$$

To study the TITO PID-tuned and robust controllers likely suitable for plasma current and horizontal position control in IR-T1 tokamak, we proceed as follows. The main point in TITO's control system is the effects of cross-couplings, which should be avoided as much as possible.

Decoupling methods have been introduced for this purpose, among which the inverted decoupling method [29,30], also named feed-forward decoupling control, is considered in our design. Note that due to the loss of observability of unstable modes, $G(s)$ can't be fully inverted. A usual block diagram for controlling the structure of TITO processes with decoupling, including $D(s)$ as the decoupling matrix transfer function, $G(s)$ as the transfer function of the controlled plant (actuator, plasma in tokamak, and sensor), P_1 and P_2 as PID

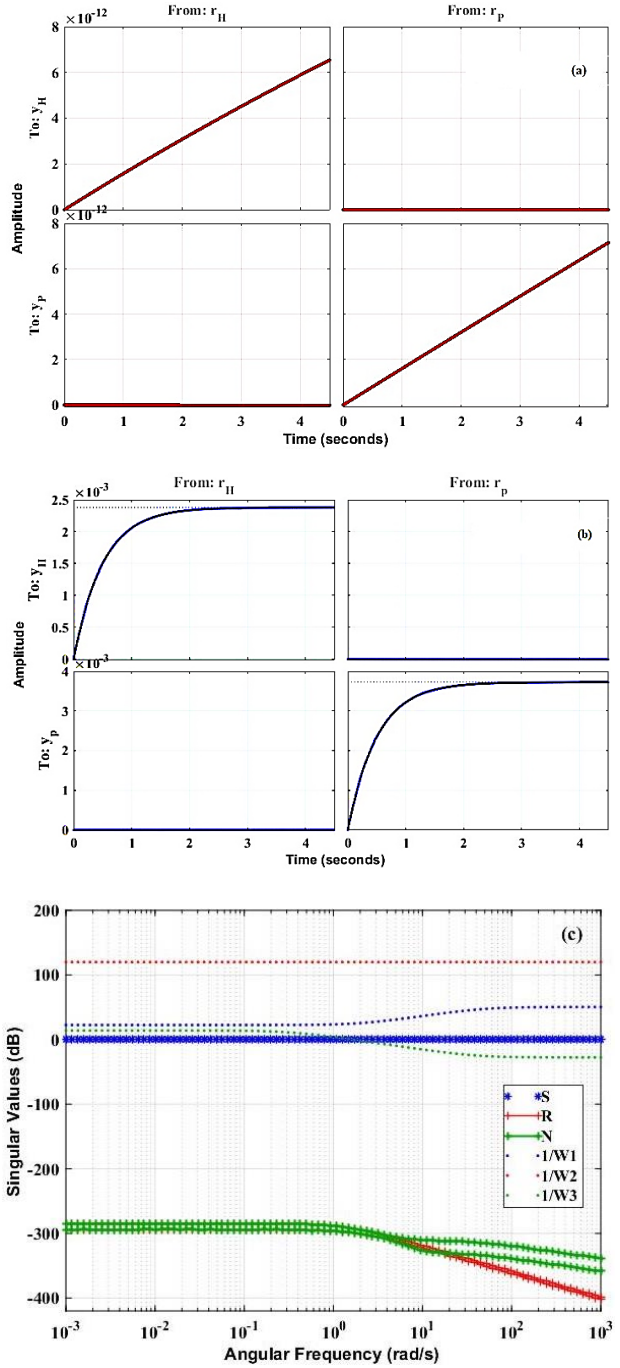

Figure. 4. Step responses of the designed TITO control system for plasma current and horizontal position control on IR-T1 tokamak, by (a) the PID-tuned and (b) the robust controllers together with (c) the robust conditions.

independent controllers designed via the above-mentioned approaches, v_1 and v_2 as independent inputs to the system, $y_1 = delta\_h$, $y_2 = delta\_I_p$ as plant outputs, and u_1, u_2 as inputs to the decoupling matrix, is shown in fig. 3(a). To proceed with the design of the robust controller $K(s)$, we considered the cascade of the decoupler and the plant [31], and then we found the gains of the controller with the H_∞ techniques. This is our suggested PID-tuned and cascaded-robust controllers [32] as shown in fig. 3(a) and 3(b).

3. Simulations

We initially discussed the closed-loop system stability. We then deal with a step reference in vertical (central transformer) field voltage as input to identify the model parameters that represent plasma horizontal position and current variations. Referring to previous work (Ref. [27]), we selected the best value for the pole of the power supply system of the vertical and central transformer coils in order to achieve better performance in terms of control and stability. The simulation results, along with the requirements of the robust controller design for plasma current and horizontal position controls, are presented in fig. 4 for the tuned-PID and H_∞ robust controllers for IR-T1 tokamak. In these figures, r_H and r_P represent the reference value for plasma horizontal position control and plasma current control, and y_H, y_P are the related outputs, respectively. Also, figures of r_P to y_H, and r_H to y_P, show plasma horizontal position variation due to change in the plasma current reference value and plasma current variation due to change in the plasma horizontal position reference value, respectively, i.e. cross-coupling of these control parameters. It can be seen that in fig. 4(b), the step response of the robust controller behaves well, and the cross-coupling for this controller (the figure of r_P to y_H, with absolute maximum amplitude 2×10^{-6}, and also r_H to y_P with maximum amplitude 2.5×10^{-8}) is very small i.e., the change in one of these control parameters does not change another output counterpart of these parameters remarkably. Also, the diagram of robust conditions, fig. 4(c), shows that the robust conditions are met. Of course, with much better performance, with maximum amplitudes from 6×10^{-19} to 10^{-15}, the cross-coupling term for the PID-tuned controller is almost zero (fig. 4(a)), which is approximately negligible compared to the robust counterparts.

Then, the PID-tuned controller performs better in removing cross-couplings. To gain a more comprehensive understanding of these performance using experimental data, which is a specific case that we will examine in the following two controllers, we will evaluate their validity and section.

3.1. Study of validity of the designed control systems: a special case

The position and current distribution of plasma depend on the magnetic field distributions around it. Magnetic pickup coils can provide information on the plasma position or boundary shift. The magnetic field distribution in the quasi-cylindrical coordinates of the poloidal and normal components around the circular cross-section plasma are given as [33]:

Table 2. Design parameters of the magnetic probes in IR-T1 tokamak.

Parameters	Value	Parameters	Value
Resistivity (Ω)	33	Turns	500
Inductance (mH)	1.5	Sensitivity (mV/G)	0.7
Wire diameter (mm)	0.1	Frequency Response (kHz)	22
Coil average Radius (mm)	3	Effective nA (m^2)	0.022

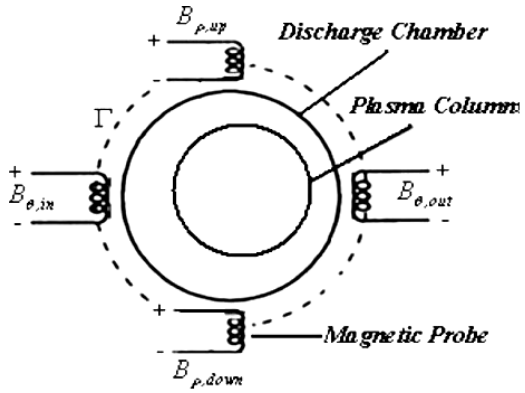

Figure. 5 Positions of the four magnetic probes on the outer surface of the IR-T1 tokamak chamber.

$$B_\theta = \frac{\mu_0 I_p}{2\pi b} - \frac{\mu_0 I_p}{4\pi R_0}\left\{\ln(\frac{a}{b}) + 1 - (\Lambda + \frac{1}{2})(\frac{a^2}{b^2} + 1) - \frac{2R_0\Delta R}{b^2}\right\}\cos\theta$$

$$B_r = -\frac{\mu_0 I_p}{4\pi R_0}\left\{\ln(\frac{a}{b}) + (\Lambda + \frac{1}{2})(\frac{a^2}{b^2} - 1) + \frac{2R_0\Delta R}{b^2}\right\}\sin\theta$$

where the Asymmetry factor is defined as:

$$\Lambda = \beta_p + \frac{l_i}{2} - 1$$

where I_p, R_0, a, b, β_p , l_i are the plasma current, major and minor plasma radiuses, minor chamber radius, poloidal beta, and internal inductance of the plasma, respectively. This relation only depends on the plasma current and magnetic field distribution. An array of four magnetic probes, with design parameters presented in table 2, was designed and constructed in IR-T1 tokamak to detect the tangential component of the magnetic field B_θ with two of them installed on the circular contour of radius $b = 16.5$ cm in angles of $\theta = 0$ and $\theta = \pi$. Also, plasma current was obtained from the Rogowski coil [34]. Two magnetic probes were also installed above, of $\theta = \frac{\pi}{2}$ and $\theta = \frac{3\pi}{2}$, to detect the normal component of the magnetic field B_r (fig. 5):

$$\langle B_\theta \rangle = B_\theta(\theta = 0) - B_\theta(\theta = \pi) \quad ,$$

$$\langle B_r \rangle = B_r(\theta = \frac{\pi}{2}) - B_r(\theta = \frac{3\pi}{2}). \qquad (9)$$

The horizontal displacement of the plasma boundary was determined by measuring $\langle B_\theta \rangle$ and $\langle B_r \rangle$ from magnetic probes (after compensation and integration of their output):

$$\Delta R = \frac{a^2}{4R_0}\left\{(\frac{b^2}{a^2} - 1) - 2\ln(\frac{a}{b})\right\} + \frac{\pi b^2}{2\mu_0 I_p}\left\{(1 - \frac{a^2}{b^2})\langle B_\theta \rangle - (1 + \frac{a^2}{b^2})\langle B_r \rangle\right\} \qquad (10)$$

To evaluate the performance of the designed controllers, we consider a particular case in which by changing the operating voltage of the vertical field coil system in IR-T1 tokamak, 3 kV, to 3.25 and 2.80 kV, the horizontal plasma displacement and the corresponding changes in the plasma current, are measured. Then their control behavior, especially the cross-coupling of the horizontal displacement and plasma current, will be investigated. Time behavior of plasma current and horizontal position for the common discharge of IR-T1 tokamak with vertical field coil voltage 3 kV, as the reference signal for the following simulations, are presented in fig. 6. The time behavior of plasma horizontal plasma displacements (with gray color) and corresponding feedback responses together with cross-couplings (with other colors) for values of vertical field coil voltage, 2.80 and 3.25 kV, are calculated and depicted in figs. 7 to 10.

Also, the enlarged part of these figures in the first part of the signal, to check the fulfillment of the control requirements considered in the manuscript as the defined main objectives (the settling time, disturbance, and cross-coupling effect rejection) together with the flat-top range of the plasma current signal i.e., around 13 milliseconds (specifically between 12-14 milliseconds) as the main phase for fusion energy production is presented. The results show a better reference value tracking and promising control of cross-coupling term, with very low oscillatory behavior, for the PID-tuned controller.

4. Results and discussion

The enlarged parts of all diagrams of figures 7 to 10 clearly demonstrate that the PID-tuned controller consistently outperformed its robust counterpart. It exhibited low oscillatory behavior, fast disturbance rejection, remarkable reference value tracking, and excellent cross-coupling control. A tokamak disruption is a significant event that can cause the plasma to lose stability, resulting in a sharp increase in plasma resistivity and a significant drop in temperature. As a consequence, a large induced electric field is produced, generating high-energy electrons known as runaway electrons. These electrons can be generated through both primary and secondary mechanisms.

Also, the enlarged part of these figures in the first part of the signal, to check the fulfillment of the control requirements considered in the manuscript as the defined main objectives (the settling time, disturbance, and cross-coupling effect rejection) together with the flat-top range of the plasma current signal i.e., around 13 milliseconds (specifically between 12-14 milliseconds) as the main phase for fusion energy production is presented. The results show a better reference value.

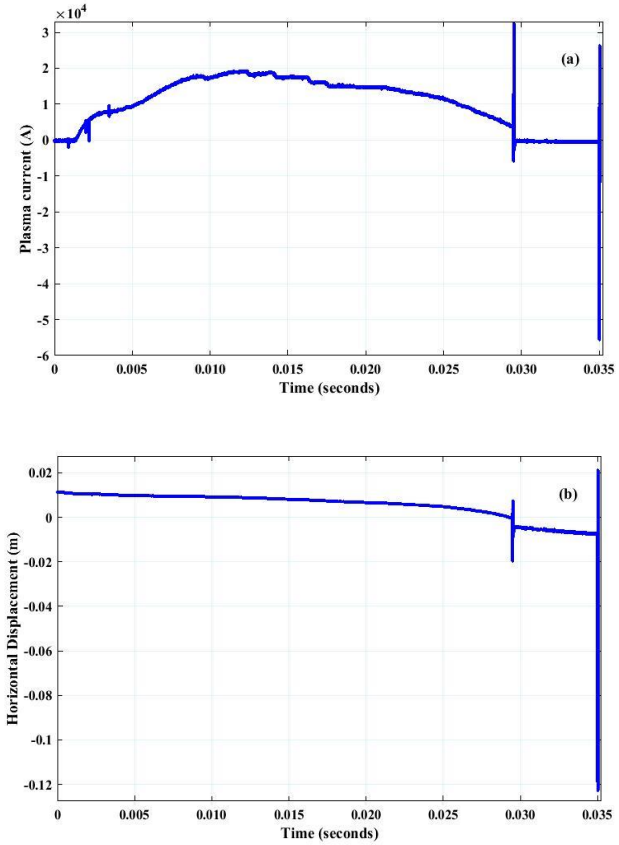

Figure. 6. Time behavior of the common discharge parameters on IR-T1 tokamak with vertical field coil voltage 3 kV, (a) plasma current, and (b) plasma horizontal displacement.

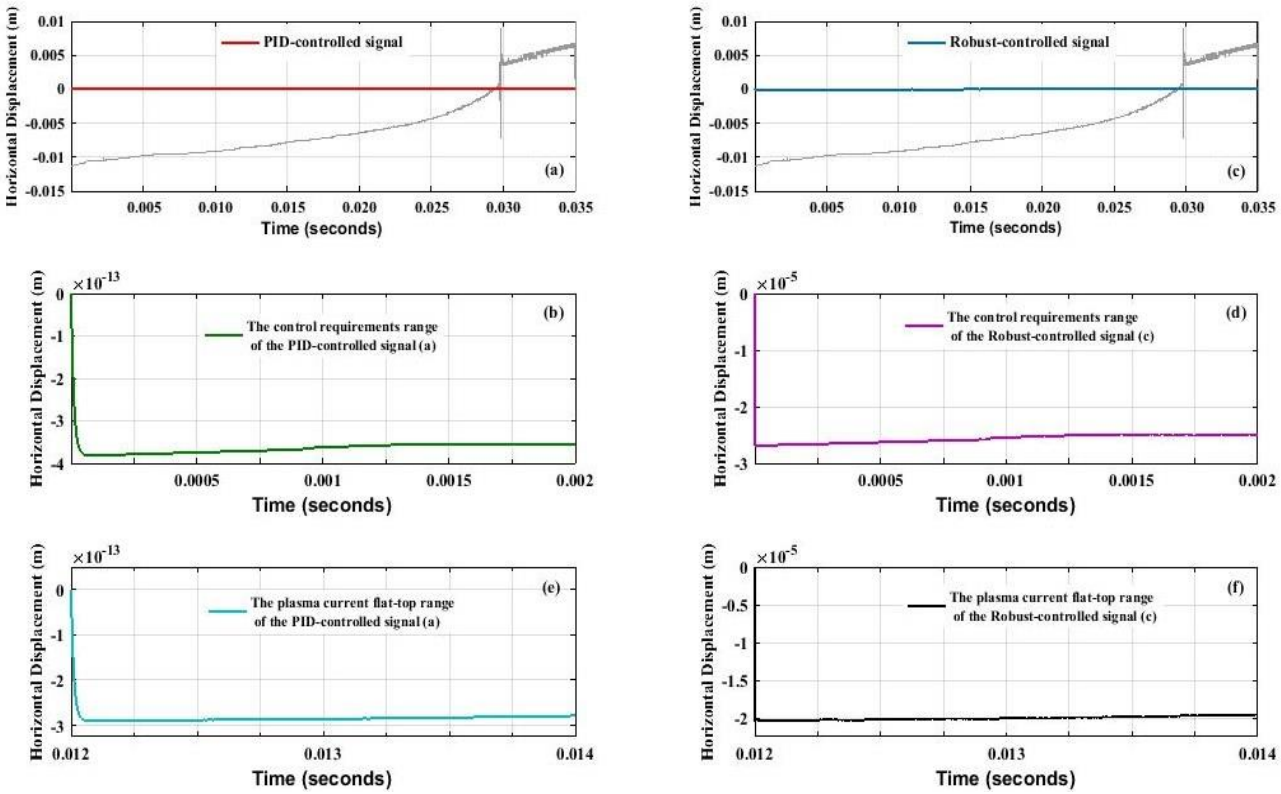

Figure. 7. (a),(c) Time behavior of plasma horizontal displacement and the designed PID-tuned and robust controller performances together with the enlarged parts, (b),(d) for the control requirements satisfaction and, (e),(f) for flat-top phase, to control of plasma horizontal displacement on IR-T1 tokamak with the vertical field coil voltage 2.80 kV.

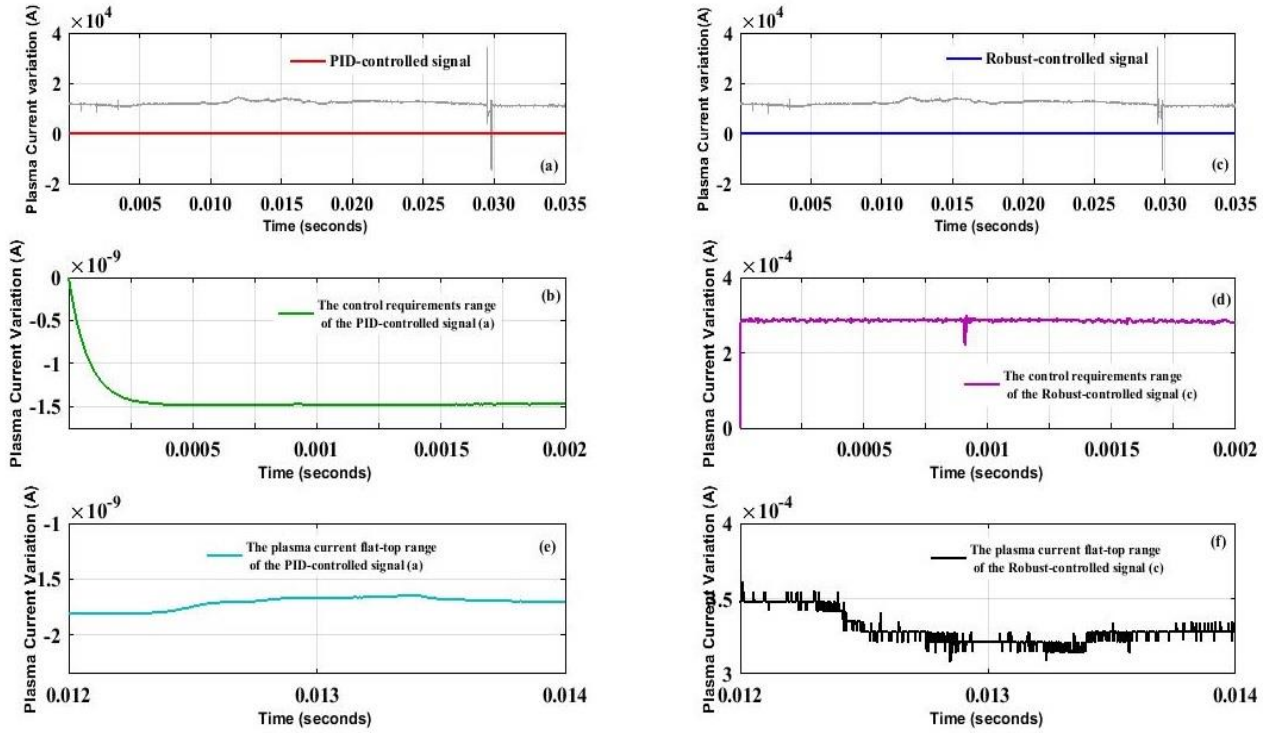

Figure. 8. (a),(c) Time behavior of plasma current variation and the designed PID-tuned and robust controller performances together with the enlarged parts, (b),(d) for the control requirements satisfaction and, (e),(f) for flat-top phase, to cross-coupling control on IR-T1 tokamak with the vertical field coil voltage 2.80 kV.

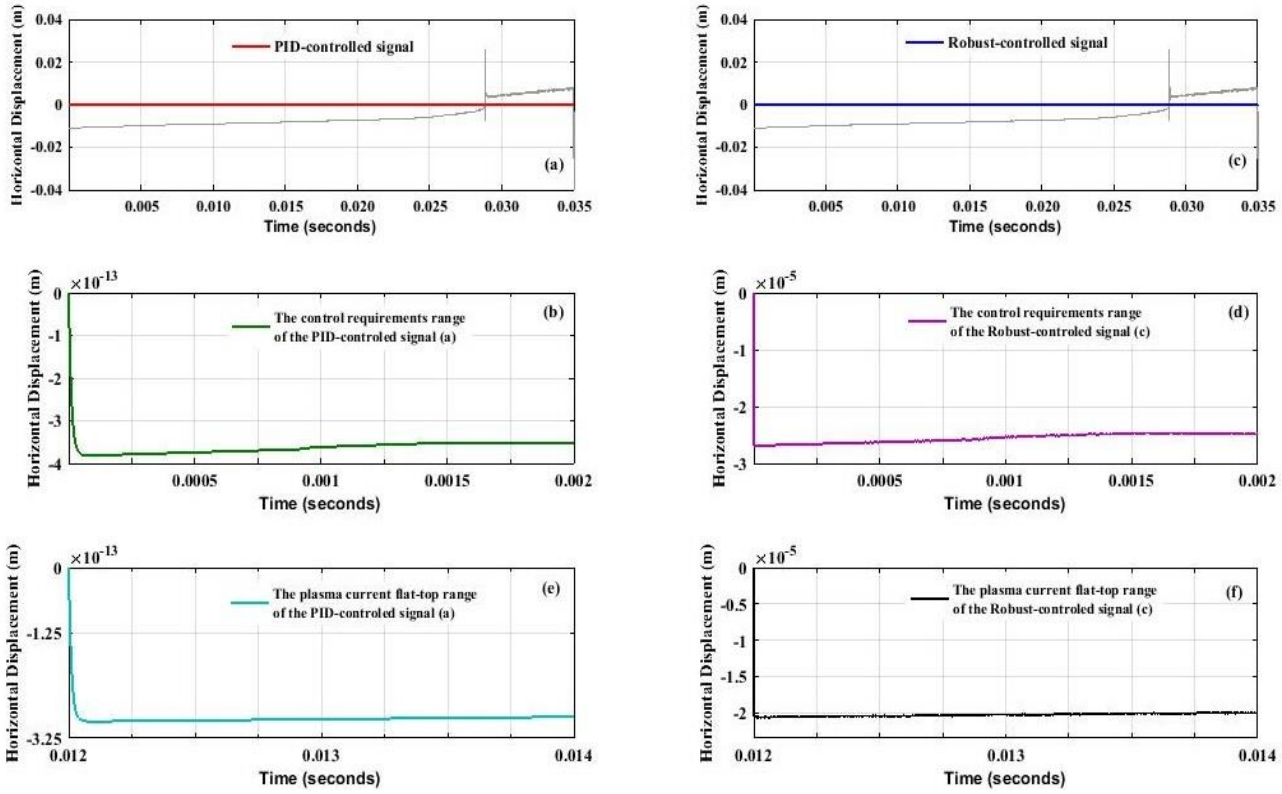

Figure. 9. (a),(c) Time behavior of plasma horizontal displacement and the designed PID-tuned and robust controller performances together with the enlarged parts, (b),(d) for the control requirements satisfaction and, (e),(f) for flat-top phase, to control of plasma horizontal position on IR-T1 tokamak with the vertical field coil voltage 3.25 kV.

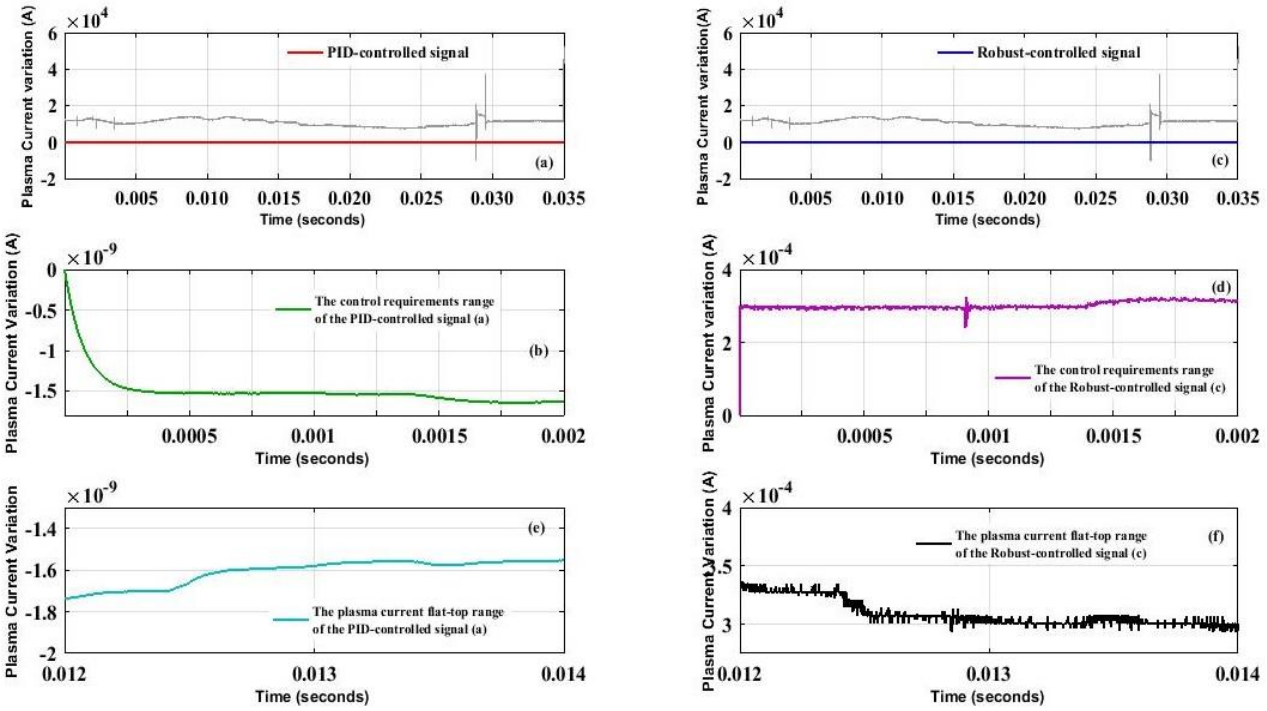

Figure. 10. (a),(c) Time behavior of plasma current variation and the designed PID-tuned and robust controller performances together with the enlarged parts, (b),(d) for the control requirements satisfaction and, (e),(f) for flat-top phase, to cross-coupling control on IR-T1 tokamak with the vertical field coil voltage 3.25 kV.

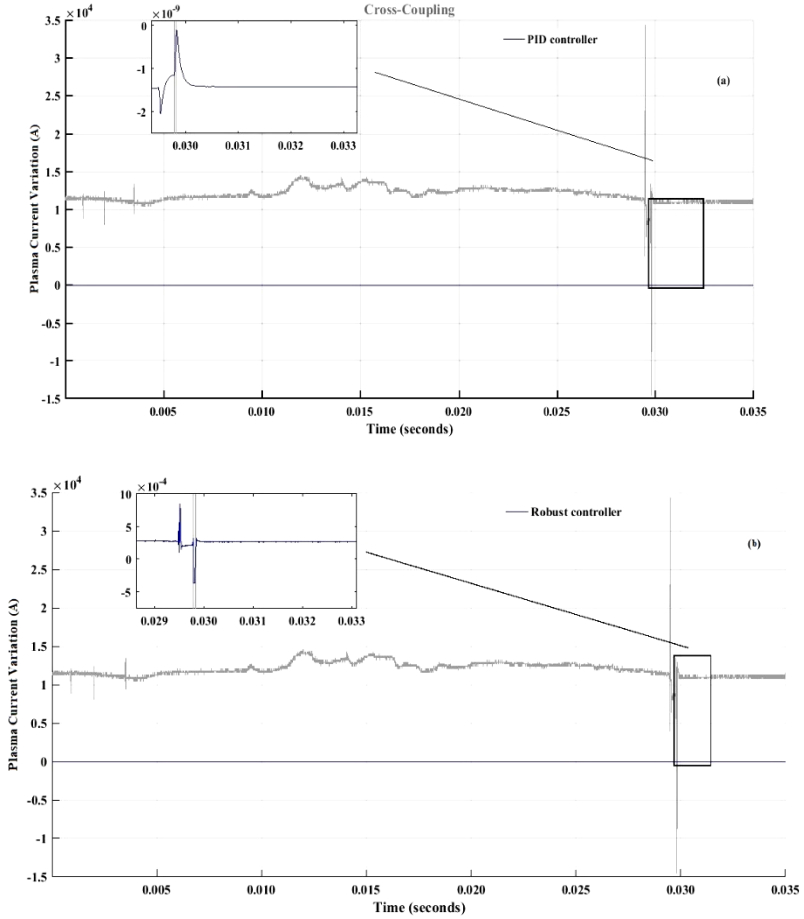

Figure. 11. (a), (b) Time behavior of the designed PID-tuned and robust controller performances in the latter times of discharge together with the enlarged part, for the control requirements satisfaction to disruption mitigation control on IR-T1 tokamak with the vertical field coil voltage of 2.80 kV.

In the primary mechanism, thermal electrons diffuse through the high-energy tail of the thermal electron population to increasingly higher energy, while the runaway avalanche effect is the secondary mechanism. Runaway electrons can cause surface damage to the first wall of the vacuum vessel and pose a serious threat. Preventing their generation and safely dispersing energy during a disruption is crucial [35]. Based on these explanations, addressing and also mitigating or eliminating these disruptions in tokamak plasma control is vital. The performance of the control system during disruptions has also been investigated based on the plasma's characteristic features.

We considered a case in the latter times, specifically a pre-disruption of plasma current in IR-T1, with 2.80 kV (fig. 11). From the perspectivet of disruption mitigation attempted through the cross-coupling control, the discrepency in performance between these two controllers during the generation of runaway electrons is significant. This generation is accompanied by an approximately exponential decay in plasma current, occuring at around 32-34 milliseconds in figures 7 and 8 and 30-32 milliseconds in figures 9 and 10.. Disruption typically follows shortly after generation of runaway electrons. We can see that the PID-tuned controller shows smooth behavior with very small amplitude oscillations. The same result as fig. 11, is obtained for the case with 3.25 kV (which is not given here).

Controlling plasma confinement in tokamak is critical, and various controllers have been designed to control plasma parameters. Due to the complex nonlinear behavior of tokamak plasmas, cross-coupling between plasma parameters, like plasma horizontal position and plasma current in IR-T1 tokamak, is inevitable.

In order to eliminate this cross-coupling, it is important to use decoupling schemes in the MIMO controllers. While numerous studies have delved into the MIMO control scheme of plasma parameters across various tokamaks, we have not encountered any that specifically address the design of PID-tuned and robust MIMO controllers with an inverted decoupling structure for tokamaks with circular cross section like IR-T1. It seems that decoupling schemes are intriguing in MIMO controller design for controlling plasma parameters in tokamaks, potentially providing enhanced decoupling between these parameters. Recent studies, such as those referenced in [36,37], could open up new horizons for advancing the application of this type of design in tokamak control systems. The obtained results, although for the specific case, will be a great guide in designing a MIMO control system that controls other parameters in addition to these two plasma parameters in tokamaks like IR-T1. Certaily, in future works, we intend to explore the performance of these two controllers across a range of experimental conditions.

5. Conclusion

Application of the cascaded robust and PID-tuned controllers to design a decoupled TITO system for controlling plasma current and plasma horizontal position in a small circular cross-section tokamak known as IR-T1, is explored. To examine the system's feedback response, a voltage-driven model is utilized. The performance of the controllers is evaluated based on the overall transfer function. Simulation results obtained using MATLAB demonstrate that both controllers effectively eliminate the cross-coupling between plasma horizontal position and plasma current. Further analasys of the two controllers using a specific experimental case reveals that the PID-tuned controller outperforms its robust counterpart in terms of control requirements and disruption mitigation. This demonstrates the viability of the designed controller. Control system design often relies on simulation results to assess performance under different conditions and optimize the design. To verify the simulation results, it is necessary to compare them with the expected behavior, analyze system stability and robustness, ensure the simulation accurately represents the system's dynamics, and confirm that the simulation software is capable of accurately simulating the control system. These enable an evaluation of the overall effectiveness of the control system design.

Based on the verified model and software used in our study, and the performance results of the designed controllers in maintaining stability, robustness, and expected dynamics of the system, we can confirm that the conditions for the verification of the study have been met. However, in order to proceed with final verification, it will be

necessary to conduct the construction, installation, and operation of these controllers in diverse plasma scenarios of tokamak.

Acknowledgment

A. Naghidokht would like to acknowledge Dr. Daniele Carnevale, for inspiring and invaluable hints about MIMO control systems design.

Conflict of interest

The authors have no conflicts to disclose.

CRediT authorship contribution

Ahmad Naghidokht: Conceptualization (lead); Methodology (lead); Writing–original draft (equal); Writing-review and editing (equal); Validation (lead); Data curation (equal); Software (equal); Visualization (equal). Morteza Janfaza: Writing–original draft (equal); Writing- review and editing (equal); Visualization (equal); Software (equal). Mahmood Ghoranneviss: Validation (supporting); Data curation (equal).

References

1. A Ogata and H Ninomiya, *Jpn. J. Appl. Phys*. **18** (1979) 825.
2. A Portone, et al., *Fusion Technol*. **32** (1997) 374.
3. G Ambrosino, et al., "*Plasma current and shape control in tokamaks using* H_∞ *and* μ*-synthesis*", in IEEE Proceedings of the Conference on Decision and Control, San Diego, California, (1997) 3697.

4. M Emami, A R Babazadeh, and H Rasouli, *Pramana; Journal of Physics* **62** (2004) 53.
5. G De Tommasi, et al., *Fusion Eng. Des.* **129** (2018) 152.
6. Y V Mitrishkin, et al., "Linear and impulse control systems for plasma unstable vertical position in elongated tokamak", in 51st IEEE conference on Decision and Control, Maui, Hawaii (2012) 1697.
7. R A Fahmy, R I Badr, and F A Rahman, *The Mediterranean Journal of Meas. Contr*. **11** (2015) 438.
8. C A Lin, "Necessary and sufficient conditions for existence of decoupling controllers", in IEEE Proceedings of the Conference on Decision and Control, New Orleans, Louisiana, (1995) 1157.
9. Q G Wang, et al., *Automat*. **33** (1997) 319.
10. F G Shinskey, "*Process Control Systems: Application, Design, and Adjustment*", McGraw-Hill, New York (1996).
11. S Skogestad and I Postlethwaite, "*Multivariable Feedback Control: Analysis and Design*", John Wiley & Sons, New York (2005).
12. K J Astrom and T Hagglund, "*PID controllers: Theory, Design and Tuning*", Instrument Society of America: Research Triangle Park, NC, (1995).
13. Y V Mitrishkin, et al., "*Plasma magnetic robust control in tokamak-reactor*", in Proceedings of the IEEE Conference on Decision and Control, San Diego, California, (2006) 2207.
14. Y V Mitrishkin, A V Kadurin, and A Y Korostelev, "*Tokamak plasma shape and current controller design in multivariable cascade system*", in IFAC World Congress, Milano, Italy (2011) 3722.
15. G Ambrosino, et al., "*A model-based controller design approach for the TCV tokamak*", in IEEE Proceedings of the International Conference on Control Applications, Trieste, Italy (1998) 202.
16. M Ariola, et al., *IEEE Trans. Contr. Syst. Technol*. **10** (2002) 646.
17. M L Walker, D A Humphreys and J R Ferron, "*Control of plasma poloidal shape and position in the DIII-D tokamak*", in IEEE Proceedings of the Conference on Decision and Control, San Diego, California (1997) 3703.
18. D A Humphreys, et al., "*Initial implementation of a multivariable plasma shape and position controller on the DIII-D tokamak*", in Proceedings of the IEEE International Conference on Control Applications, Anchorage, Alaska (2000) 412.
19. R Albanese, et al., "*A MIMO architecture for integrated control of plasma shape and flux expansion for the EAST tokamak*", in IEEE Conference on Control Applications, Buenos Aires, Argentina (2016) 611.
20. W Shi, et al., "*Multivariable multi-model-based magnetic control system for the current ramp-up phase in the National Spherical Torus Experiment (NSTX)*", in 50th IEEE Conference on Decision and Control and European Control Conference, Orlando, Florida (2011) 2632.
21. L Boncagni, et al., "*Performance-based controller switching: An application to plasma current control at FTU*", in 54th IEEE Conference on Decision and Control, Osaka, Japan (2015) 2319.
22. G Ramogida, et al., *Nucl. Mat. Energy* **12** (2017) 1082.
23. A Naghidokht, et al., *Fusion Eng. Des*. **107** (2016) 82.
24. S Meshkani, M Ghoranneviss and Ch Rasouli, "*Recent MCF Activities in Iran*", in 23rd IAEA Technical Meeting on Research Using Small Fusion Devices, Santiago, Chile (2017) 1-88.
25. Z. Goodarzi, M. Ghoranneviss, and A. Salar Elahi, *J. Fusion Energy* **32** (2013) 103.
26. M Ariola and A Pironti, "*Magnetic Control of Tokamak Plasmas*", Springer-Verlag, London (2008).
27. Y Suzuki, et al., *Jpn. J. Appl. Phys*. **16** (1997) 2237.
28. G Balas, et al., " *-Analysis and Synthesis Toolbox: for Use with MATLAB, User's Guide version 3*", The MathWorks Inc. (1998).
29. E Gagnon, A Pomerleau, and A Desbiens, *ISA Trans*. **37** (1998) 265.
30. P Y Chen and W D Zhang, *ISA Trans*. **46** (2007) 199.
31. L Boncagni, et al., *Fusion Eng. Des*. **88** (2013) 1109.
32. A Naghidokht, "*MIMO IR-T1: MATLAB M-File for designing of a decoupled Multiple-Input Multiple-Output (MIMO) controller for plasma current and horizontal position in IR-T1 tokamak*", Mendeley Data, V. 2, Dataset, (2022) https://doi.org/10.17632/khwsrw8hy6.1.
33. H. Niomiya and N. Suzuki, *Jpn. J. Appl. Phys*. **21** (1982) 1323.
34. M Emami, M Ghoranneviss, and R Tarkeshian, *Fusion Eng. Des*. **83** (2008) 684.
35. A. Salar Elahi and M. Ghoranneviss, *J. Fusion Energy* **33** (2014) 242.
36. A P V d A Aguiar, G Acioli Júnior and P R Barros, *J. Control. Autom. Electr. Syst*. **32** (2011) 830.
37. R H Naik, D V A Kumar, and P Sujatha, *Ain Shams Eng. Journal* **11** (2020) 343.